5th Multiphase Flow Journeys
May 17th-18th, 2019, Rio de Janeiro, RJ, Brazil

JEM-2019-XXXX (XXXX is the manuscript number, times new roman, centered, bold, size 14 **)**

MULTI-PHASE PNEUMATIC FLOW ANALYSIS FOR SHOT PEENING USING EULER-LAGRANGE APPROACHES

Robinson Imaiti Mashiba
robinsonmashiba@gmail.com
Flavius Portella Ribas Martins
Escola Politécnica da Universidade de São Paulo
flavius.martins@usp.br

Abstract. *In this article we develop a Euler-Lagrangian model representing the two-phase flow along the pneumatic conveying pipeline of a shot peening equipment. Simulations of this model indicated that nozzle throat section is mainly responsible for the outlet particle velocity field.*

Keywords: *multiphase flow, pneumatic conveying, shot peening*

1. INTRODUCTION

Peen forming is a technique widely used in industrial activity for shaping metallic sheets and panels. It is based on the application of a jet of small metallic spheres (shot) propelled by compressed air against the surface of the part to be conformed. The greater the pressure difference along the pneumatic conveying line (consisting of an abrasive hose connected to a nozzle), the larger the average impact velocity and the resulting deformation of the part.

Friction between the shot and the inner walls of the pipeline, turbulence resulting from the shot-fluid interaction and abrupt variations in the curvature of the pipeline cause gradual loss of load along the pneumatic conveying line. Moreover, at the interfaces separating the solid and gaseous phases, discontinuity occurs in the values of the physical properties of the flow, increasing the difficulty of the analysis.

Much of the modeling difficulty of this class of flows concentrates on the physical behavior of the multiple and mobile interfaces that separate the phases. Although many advances have already been achieved in the study of solid-gas flows (Portela et al., 2003; Zhu et al., 2008), combinations of geometric characteristics and physical properties give rise to many questions still to be answered.

To model multiphase flows, both Eulerian and Lagrangian approaches may be coupled; so, multiphase Euler-Euler and Euler-Lagrangian models are commonly found in the literature (
ZHU H.P et al , 2008,KUSSIN J.,2002, FRANK TH.,1993). During the modeling, three essential points must be investigated: 1) interactions among the phases and the external environment; 2) number of Stokes; 3) volumetric fractions.

Table 1 shows the four types of interactions that can be considered in the models.

Table 1: Coupling between the phases

	Iterations between phases			
	Fluid → Dispersed	Fluid ↔ Dispersed	Disturbance in flow and surrounding particles	Particle collision
One - Way	Ex: Drag on particles			
Two - Way	Ex: Drag on particles	Ex: Loss of fluid load		
Three - Way	Ex: Drag on particles	Ex: Loss of fluid load	Ex: Reduction of drag by the movement of one particle in the esteria of another	
Four - Way	Ex: Drag on particles	Ex: Loss of fluid load	Ex: Reduction of drag by the movement of one particle in the esteria of another	Ex: contact force and drag between particles

The Stokes number is defined as

$$S_T = \frac{\tau_p}{\tau_F} \qquad \text{(Eq. 1)}$$

Where τ_F is a fluid constant time and τ_P is the particle relaxation time, given by:

$$\tau_p = \frac{\rho_p d_p^2}{18\mu_q} \quad \text{(Eq.2)}$$

Where d_p is the particle diameter, ρ_p is the particle density and μ_q is the fluid kinematic viscosity.

High Stokes numbers indicate that the discrete phase has much inertia, tending to follow its own dynamics, being little affected by the continuous phase velocity field (Hinds, 1982), but causing perturbations and load loss in the continuous medium. This is a 'two-way' interaction.

Volumetric fraction is also a critical factor (see Fig.1). By increasing the fraction of the discrete phase, disturbances are introduced into the fluid medium (three-way interaction); in the limit, when the discrete phase becomes quite compact, the friction between the particles becomes a dominant force (four-way interaction)

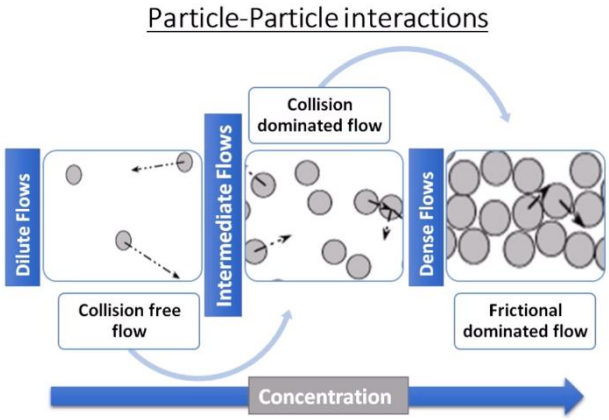

Figure 1: Interaction between particles, Source: Course of Computational Modeling of Multiphase Flows with ANSYS CFD.

It can be observed that the flow can be analyzed considering several forms of interaction of the medium, however it is remarkable that when considering a four-way interaction in the simulation the answer will be more precise, however, it will require a computational cost greater than the simulation in two -way due to the increase of physical phenomena in the analysis, in this way it is very important to analyze the limitations of these models and the applicability in the case under study, in order to obtain a better solution with a lower computational cost.

2. MULTIPHASIC FLOW

The multiphase flow consists of a flow of distinct phases, these phases being defined as an identifiable fraction of matter, which has a characteristic inertial response when interacting with the flow and with the potential field in which it is immersed, in this way solid particles of the same material, can be defined as distinct phases because they have different sizes (Crowen et al, 1998)

This flow is common in nature and in various engineering areas, such as oil extraction, pneumatic transport equipment, internal combustion engines, among others. In this paper, we present the results obtained from the modeling and simulation of multiphase flows, which have been the subject of continuous research (Huber et al., 1999, Saffman et al., 1965, Salman et al. 2005, Morsi et al., 1972). Sommerfield et al., 1998 emphasized that the great complexity of this type of flow lies in the behavior of the phase separation interfaces, which interfaces can be multiple, deformable and mobile, producing discontinuity zones in the values of the physical properties of the flow, due to the great variety of classes and interactions internal to the multiphase flow and given its importance in the field of research, numerous expressions and combinations of mathematical methods were created in order to achieve a simplification in the resolution of this physical phenomenon, separating them into Lagrangean approaches and Eulerian approaches.

3. EULERIAN - LAGRANGEAN MODEL EQUATIONS

In the Eulerian-Lagrangian approach the phases interact through drag forces ($\vec{F}_p^{drag}$) and source terms (S_q). The continuous phase is provided by the Navier-Stokes equations plus the source term, as already described in the previous topic. The dispersed phase time evolution is obtained through the integration of the Newton's Second Law for each particle (Eq.5) (ZHU et al. al., 2008), assuming, by hypothesis, that the effect of rotational motion is negligible.

$$m_p \frac{d\vec{v}}{dt} = \sum \vec{F}_{pq}^{c} + \sum \vec{F}_{pk}^{nc} + \vec{F}_p^{g} + \vec{F}_p^{drag} \quad \text{(Eq.3)}$$

Where

$$\vec{F}_p^{drag} = \frac{1}{2}\left(\frac{C_d \pi d_p^2}{4}\right) p_q (u - v)|u - v| \quad \text{(Eq.4)}$$

Gas flow is naturally modeled by adopting Euler's approach. For this, the Navier-Stokes equations are solved in connection with the k-ε turbulence model or, with the Reynolds Stress Model (RSM) (Jones and Musonge 1988, Jones, 1994). It is assumed that the interaction of the gas phase with the dispersed medium is represented by the drag forces and the turbulence effects.

The equation of continuity, representing conservation of mass, is written as:

$$\frac{\partial \rho_g}{\partial t} + \nabla.\left(\rho_g \vec{u}_g\right) = S_m \quad \text{(Eq.5)}$$

And the equation represented by the conservation of the momentum is :

$$\frac{\partial}{\partial t}\left(\rho_g \vec{u}_g\right) + \nabla.\left(\rho_g \vec{u}_g \vec{u}_g\right) = -\nabla p + \rho_g \vec{g} + \vec{F}_s \quad \text{(Eq.6)}$$

Where ρ_g, u_g, S_m, $\rho_g \vec{g}$, p and $\vec{F}_S$ are respectively Specific gas mass, Gas velocity (air), Source term due to interaction with the dispersed, Gravitational body force, Static pressure and External body forces (for example, forces that arise from interaction with the dispersed phase)

3.1 INTERACTION WITH THE WALL

According to Salman et al., 2005, in the general case the contact of a sphere on a solid surface is a complex process, involving the effects of elastic and inelastic properties, together with the interfacial friction that leads to a combination of adhesion, slipping and sliding, in this way several studies were developed in this variable (NING A., 2001, KHARAZ AH, 2001, SALMAN AD, 1999), arriving at some simplifications. Salman et al., 2005, noted that as the angle between the particle and wall trajectory is low, the particle slides and can be considered as a simple rigid body model, a study by Salman et al., 1997 observed that the velocity normal impact on the wall of the tube is typically the $v_V = 1{,}1\,\frac{m}{s}$, of energy loss during the impact is very small, and it is possible to adopt the elastic collision hypothesis e_$e_N = 1$, according to Kharaz, 2001, in the collision there are two fundamental parameters, the tangential and normal return coefficient, in which the tangential restitution coefficient can be described as:

$$e_t = 1 - 2\mu tan\alpha_i \quad \text{(Eq.7)}$$

Kharaz also observed the rotation transmitted due to the impact and can be described as the following equation:

$$\omega_i - \omega_r = \frac{5V_{ij}}{2r}(1 - e_t) \quad \text{(Eq.8)}$$

In order to observe the phenomenon of sliding between wall and particle during the impact, Ning developed a criterion to identify the possibility of this phenomenon during the impact, so that if the expression is real, the collision slip will occur:

$$\cot(\alpha_i) + \frac{r\omega_i}{V_{ni}} \geq 6\mu \quad \text{(Eq.9)}$$

Where μ, α_i, ω_i, ω_r, V_{ij} and V_{ni} are respectively coefficient of friction, angle of collision of the particle with the wall, speed of rotation before impact, rotation speed after impact, impact tangential velocity and normal impact speed

3.2 LIFT FORCE

According to Salman et al., 2005, the lift force is due to the action of two main factors, the velocity gradient in the particle and the rotation of the particle. It can be decomposed into two terms:

$$F_L = F_{L\Delta v} + F_{LM} \quad \text{(Eq.10)}$$

Where $F_{L\Delta v}$ and F_{LM} are respectively Force due to the velocity gradient and Force due to rotation (Magnus Force)

Shaffman in 1965 equated, for low Reynolds numbers, the velocity gradient effects on the lift force ($F_{L\Delta v}$) of an internal particle to the flow, in 2001 Safman Li and Ahman studied the dispersion of spherical particles in a turbulent flow, generalizing the expression of Shaffman, 1965, in the following equation:

$$\vec{F} = \frac{2kv^{\frac{1}{2}}\rho d_{ij}}{\rho_p d_p((d_{lk}d_{kl}))^{\frac{1}{4}}}(\vec{u} - \vec{u}_p) \quad \text{(Eq.11)}$$

Where $K = 2.594$ and d_{ij} is the deformation tensor

In the case of the force due to rotation (F_{LM}), also known as magnus force, we have the following expression (CROWE C. ET AL, 1998):

$$F_{RL} = \frac{1}{2}A_P C_{RL}\rho_f . \frac{|\vec{V}|}{|\vec{\Omega}|}(\vec{V} \times \vec{\Omega}) \quad \text{(Eq.12)}$$

Where C_{RL} is known as the rotational lift coefficient, it can be calculated by a Role-dependent Reynolds number expression (Re_ω) and the Reynolds number of the particle Re_P, being validated for $Re_p < 2000$ and proposed by Osterle and Bui Dinh, 1998:

$$C_{RL} = 0.45 + \left(\frac{Re_\omega}{Re_p} - 0.45\right)\exp(-0.05684 Re_\omega^{0.4} Re_p^{0.3}) \quad \text{(Eq.13)}$$

3.3 DRAG LAW (SPHERICAL PARTICLE)

In the interactions between continuous and dispersed phases the influence of the drag force is determinant for the prediction of the velocity field and the trajectory of the particles. In pneumatic flows it is known that this force is the result of the relative velocity between the air current and the particles, and can be expressed as an equation in function of this relative velocity and the geometry of the particle:

$$F_d = \frac{C_d}{2}\rho_g\left(U_g - U_p\right)^2 A_p \quad \text{(Eq.14)}$$

Where: C_d, ρ_g, U_g, U_P and A_p are respectively, coefficient of drag, specific gas mass, gas velocity, particle velocity (shot) and particle surface area

According to Zenz and Othmer (1960), for small values of Reynolds number ($Re \sim 0{,}1$), one can adopt the linear approximation of Stokes to the coefficient of drag, that is, to adopt:

$$C_d = \frac{24}{Re} \quad \text{(Eq.15)}$$

In case of high Reynolds number flows ($Re > 10^8$), it can be assumed that the drag coefficient (C_d) is constant and close to 0.4 (MORSI et al, 1972).

Considering that, in many solid-gas flows of interest, the Reynolds number lies in the intermediate range between the values indicated above, Alexander et al. (1972) lifted the drag coefficient curve as a function of the Reynolds number from a series of measurements in solid-gas flows in which the dispersed phase was composed of spherical particles

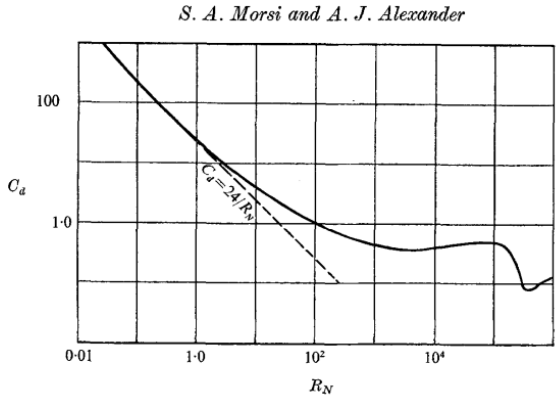

Figure 2: C_d x R_{eN} experimental curve (Source: Morsi, S. A. & Alexander, A. J.,1972)

Using the graph of the previous, we arrive at the following expression of the coefficient of drag:

$$C_d = \frac{k_1}{R_N} + \frac{k_2}{(R_N)^2} + k_3 \quad \text{(Eq.16)}$$

Morsi and Alexander, 1972 divided the experimental curve into Reynolds number intervals by finding the constants k for each chosen range, the width of the chosen region was adjusted so that the discrepancy between the analytical equation and the experimental curve was insignificant. coefficients k_1, k_2 and k_3 presented in Table 2.

Table 2: Table of constants for determination of drag coefficient (Source: Morsi, S. A. & Alexander, A. J.,1972)

k1	k2	k3	Numero de Reynolds
24,00	0,00	0,00	Re < 0,1
22,73	0,09	3,69	0,1 < Re < 1,0
29,17	-3,89	1,22	1,0 < Re < 10,0
46,50	-116,67	0,62	10,0 < Re < 100,0
98,33	-2778,00	0,36	100,0 < Re < 1000,0
148,63	-47500,00	0,36	1000,0 < Re < 5000,0
-490,55	578700,00	0,46	5000,0 < Re < 10000,0
-1662,50	5416700,00	0,52	10000,0 < Re < 50000

4. TURBULENCE MODEL ($k-\omega$ SST)

Based initially on Wilcox's model, 1998, the model consists of an empirical model based on two transport equations, one for the turbulent kinetic energy (k) and the other for the specific dissipation rate (ω), the model evolved in the course (k) and (ω), improving the accuracy of the model in solutions close to the wall.

The k-ω sst models modifies the turbulent viscosity formulation to solve turbulent shear stress transport effects, in this way the model has become more accurate and reliable for a wider range of flow classes than the previous model, among them models of compressible flows.

Then we have that the turbulent viscosity for this model is:

$$\mu_t = \frac{\frac{\rho k}{\omega}1}{\max\left[\frac{1}{\alpha^*}, \frac{SF_2}{a_1\omega}\right]} \quad \text{(Eq.17)}$$

Where α^* is a turbulent viscosity term, and is given by:

$$\alpha^* = \frac{\alpha_\infty^*\left(\alpha_0^* + \frac{Re_t}{R_k}\right)}{1+\frac{Re_t}{R_k}} \quad \text{(Eq.18)}$$

Where: $Re_t = \frac{\rho k}{\omega}$, $R_K = 6$, $\alpha_0^* = \frac{\beta_i}{3}$ e $\beta_i = 0.072$, it is worth mentioning that for high Reynolds $\alpha^* = \alpha_\infty^* = 1$

The term S of (Eq.19) represents the magnitude of the strain rate and the term F_2 da (Eq.19) is given by:

$$F_2 = \tanh(\emptyset_2^2) \quad \text{(Eq.19)}$$

$$\emptyset_2 = \max[\frac{2\sqrt{k}}{0{,}09\omega y}, \frac{500\mu}{\rho y^2 \omega}] \quad \text{(Eq.20)}$$

Where y is the distance to the surface

5. ANALYSIS AND MODEL

The pneumatic conveying pipeline, composed by ducts, elbows and a venturi nozzle, is illustrated in Fig.2

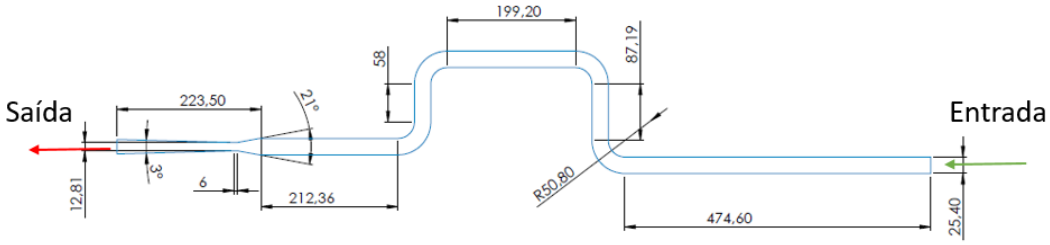

Figure 3: Schematic drawing of the simulated model

As we are dealing with a multiphase flow with $S_T > 1$ we start the analysis with a 'two-way', Euler-Lagrange model, assuming that in the walls the particles undergo reflections and that the flow has low volumetric fraction ($\alpha_p < 10\%$) as referred in ANSYS (2016)). The results of Table 2 confirm this last hypothesis.

Table 3: Volumetric fraction calculation

Number of particles entering (n/s)	4,20E+00
Particle volume (m^3)	9,04779E-10
Volumetric particle flow (m^3/s)	3,80E-09
Volumetric flow rate of air (m^3/2)	0,025
Volumetric fraction of the particle α_p	1,50E-07

Table 3 shows the list of the essential hypotheses used in the model.

Table 4: input conditions

Model	Continuos phase		Dispersed phase	
Euler - Lagrange	equation	Navier-Stokes	Equation	Second law of newton
Two-Way	Forces	drag force (SPHERICAL PARTICLE, Morsi and Alexander),Lift force (Magnus Force),Impact force with wall (Hertz)	Particle	S-230
	Turbulence model	k-w (SST)	Diameter (mm)	0,6
	Gás model	Gás ideal	Speed (m/s)	0
	Pressão de entrada	20 PSI	Mass Flow (Kg/s)	3,00E-05
			Density (Kg/m^3)	7890

Firstly we simulated the single-phase air flow, admitting that no particles are inserted in the pipeline. The resulting velocity field is shown in Figure 3.

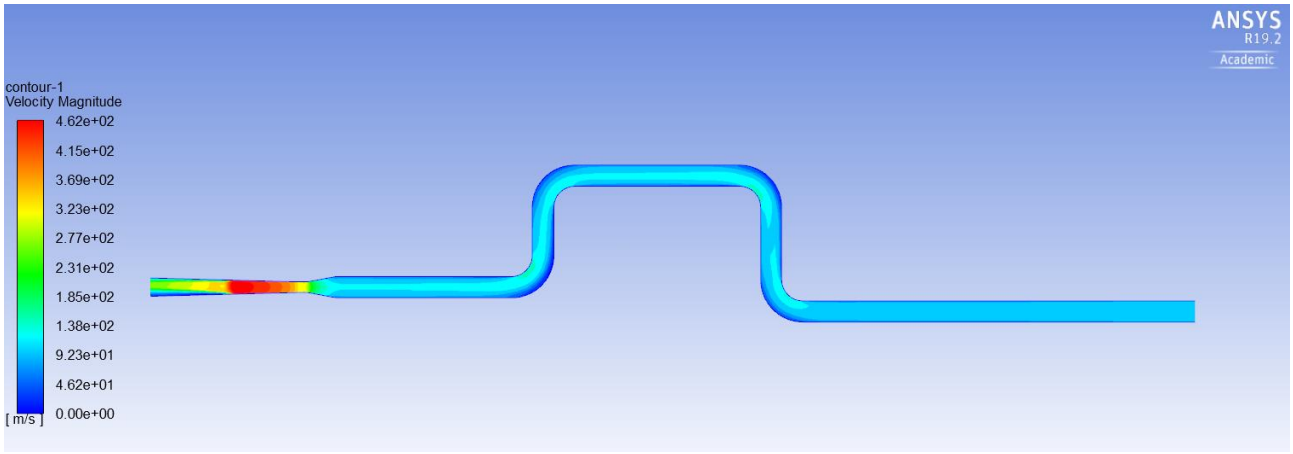

Figure 4: single phase, air velocity field

It can be observed in the response that there is a region of shock in the system, also it is noticed that after the effect of the shock the flow is not symmetrical with respect to the central axis, this can be due to the sudden variation of speed in the simulation being able to propagate small errors computational, this can be better analyzed from a suitable refinement of the mesh in the region of the phenomenon.

Thus, in order to obtain greater safety in the results, the velocity values in the shock region and in the nozzle outlet were calculated analytically, considering the isoentropic nozzle hypothesis, arriving at the following results:

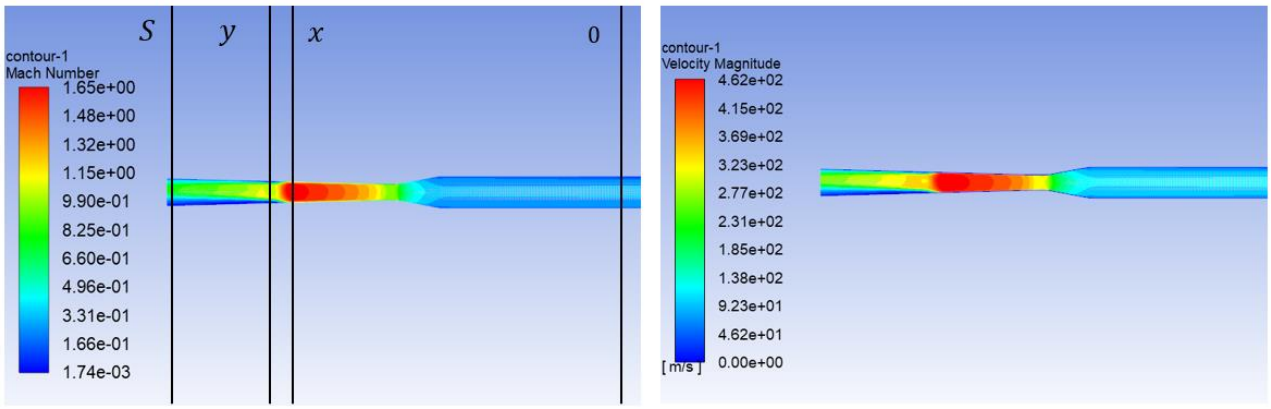

(a) (b)

Figure 5:Speed response in the nozzle,(a) representation of the analytically calculated regions mach number before and after the shock,(b) velocity before and after the shock

input hypothesis	
nozzle	M>1
perfect gas	1,4
Mac x	1,65
Po (pa)	68947,6
T0 (K)	300
calculation M>1 (antes do choque)	
Mac y	0,65
Px (pa)	15057,80
Tx (K)	194,24
Ax/A*x	1,29
Py (pa)	45317,70
Ty	276,36
Poy (Pa)	60397,30

Subsonic diffuser	M<1
A/A*y	1,132
Py/Poy	0,750
AS/A*x	1,100
AS/Ax	1,300
AS/A*S	1,253
PS	49104,989
TS	282,773
CS	337,073
mach number on the output	
M<1	M>1
0,55	1,60

	analytical result		
region	Pressure (pa)	speed of sound (C)	output speed (m/s)
0	68947,60	347,19	0,00
X	15057,80	279,36	460,95
y	45317,70	333,23	217,92
S	49104,99	337,07	186,04

Figure 6: Analytical results of the calculation in the region of the shock

It can be noted in Figure 6 that mach number and calculated velocities are very close to the one presented in the simulation, showing that the simulation is not out of the expected. By introducing into the pipeline inlet section solid particulate under the conditions indicated in ,Table 4 and using the velocity field generated in the previous step (Fig.3), we finally obtained the velocity fields shown in Figure 7 and Figure 8 concerning the continuous and disperse phases, respectively

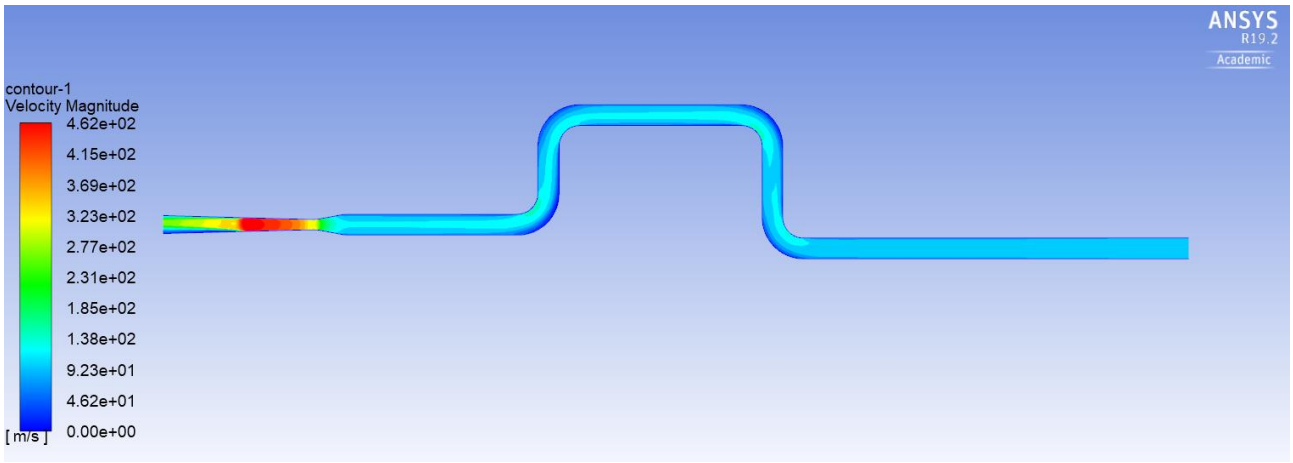

Figure 7: Continuous phase velocity field affected by the disperse phase.

Comparing Figure 5Figure 6 and Figure 7, we observe a velocity drop in the nozzle throat, of the order of 3 m / s, resulting from the dissipation of the turbulent energy of the multiphase flow.

Analyzing the result of the dispersed medium we have **Error! Reference source not found.** :

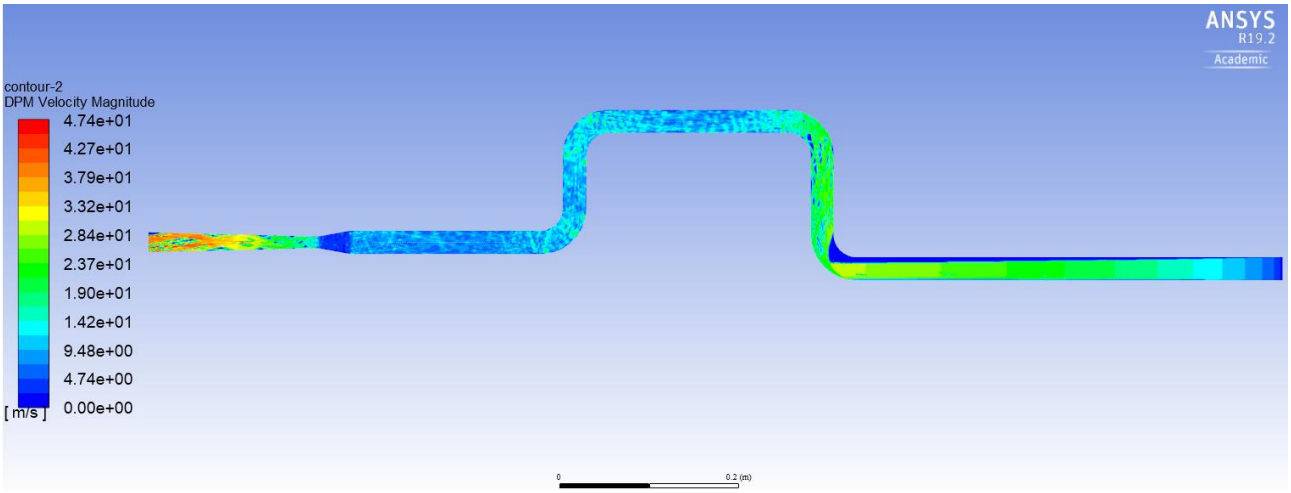

Figure 8: Disperse phase velocity field affected by the continuous phase.

It is noted by the answer that the presence of curves in the pneumatic line generates a loss of energy in the dispersed phase this occurs due to the interactions of inelastic impact between the wall and the particles. At the entrance of the nozzle is also seen a loss of speed due to this same phenomenon, we can also admit that the interaction with air in this region is not the result of the decay of the velocity of the dispersed medium, because the air velocity in this region is increasing as shown by Figure 7, thus, the velocity drop identified in the dispersed medium at the mouthpiece inlet is solely due to the particle-wall interactions.

Analyzing the behavior of the medium dispersed in the ventur, we have seen that its throat velocity is $V_{p,throat} = 23{,}7\ m/s$, reaching an output velocity equal to $V_S = 47{,}4\ m/s$, it is also seen (Figure 8) that the greatest velocity gain occurs in the region between the throat of the nozzle and the shock, because in this region the air is accelerated by the nozzle reaching values above the velocity of the sound $M = 1{,}65$ (Figure 5), thereby increasing the drag on the particles.

Another characteristic of the dispersed phase behavior in the nozzle is that after the shock its velocity remains constant,, while the speed of the air reaches more than 450 m/s in the same section but drops to $230\ m/s$ after the crash.This can be explained considering Eq.1: as $\tau_p \gg \tau_F$, then $S_t \gg 1$ (Eq.1) and the disperse phase response is slow, the acceleration of the particle is low , which is why its velocity remains constant until the nozzle exit.

6. CONCLUSION

In this paper, we analyze a pneumatic conveying pipeline using the Euler-Lagrangian approach. The simulations showed that, despite the dispersed medium being influenced by the duct geometry, for a dispersed stream with low volumetric fraction and Stokes numbers sufficiently high, the throat to the outlet of the venturi nozzle is the region that most influence the speed of the particles, and is little influenced by the continuous medium when it abruptly varies its velocity.

We will continue to analyse this the problem adopting a Euler-Euler approach. Finally we will establish a model verification criterium based on a statistical analysis concerning the velocity and pressure fields issued by those two models.

7. REFERENCES

Anderson T. B. and Jackson. R. "A Fluid Mechanical Description of Fluidized Beds". I & EC Fundam. 6. 527–534. 1967

ANSYS FLUENT, Theory Guide, 2016.

Crowe C., Sommerfield M.., and Yutaka Tsuji. Multiphase Flows with Droplets and Particles. CRC Press. 1998.

Frank Th., Schade F.P., Petrak D ., Numerical simulation and experimental investigation of a gas–solid two-phase flow in a horizontal channel, International Journal of Multiphase Flow, 19 (1993), pp. 187-198

Hinds, W.C., Aerosol Technology: Properties, Behavior, and Measurement of Airborne Particles. John Wiley and Sons, New York.

Kharaz A.H., Gorham D.A., Salman A.D., An experimental study of the elastic rebound of spheres, Powder Techol.,120 (2001),pp. 281-291

Kharaz A.H., Gorham D.A., Salman A.D., Accurate measurement of particle impact parameters, Meas.Sci. Technol., 10 (1999), pp.31-35

Kussin J., Sommerfeld M., Experimental studies on particle behaviour and turbulence modification in horizontal channel flow with different wall roughness, Experiments in Fluids, 33 (2002), pp. 143-159

Li A., Ahmadi G., "Dispersion and Deposition of Spherical Particles from Point Sources in a Turbulent Channel Flow". Aerosol Science and Technology. 16. 209–226. 1992

Moorisey, J.P., 2013, “Discrete Element Modelling of Iron Ore Pellets to Include the Effects of Moisture and Fines”. PhD Thesis: Institute for infrastructure and Environment School of Engineering. Edinburgh.

Morsi, S. A., Alexander, A. J. An investigation of particle trajectories in two-phase flow systems., Journal of Fluid Mechanics, Volume 55 , Issue 02 , September 1972, pp 193 ¬ 208

Ning A., Elasto-Plastic impacto f fine particle and fragmentation of small agglomerates, Phd Thesis, The University of Aston in Birmingham, 1995

Oesterle B. and Bui Dinh T., "Experiments on the lift of a spinning sphere in a range of intermediate Reynolds numbers". Exp. Fluids. 25. 16-22. 1998.

Patankar, SV., 1980. Numerical Heat Transfer and Fluid Flow. New York,1980.

Portela, L. M.; Oliemans, R. V. A. Eulerian-Lagrangian DNS/LES of Particle-Turbulence Interations in Wall-Bounded flows. International Journal for Numerical Methods in Fluids, V. 43, pp. 1045-1065, 2003.

Portela, L.M., Oliemans, R.V.A., “Possibilities and Limitations of Computer Simulations of Industrial Turbulent Dispersed Multiphase Flows. Flow turbulent Combust, p. 384-403, 2006.

Saffman P. G., "The Lift on a Small Sphere in a Slow Shear Flow". J.Fluid Mech. 22. 385–400. 1965.

Wilcox D. C.. Turbulence Modeling for CFD. DCW Industries, Inc. La Canada, California. 1998.

Salman A. D., Gorham D. A., Szabó M., Hounslow M.J., Spherical particle movement in dilute pneumatic conveying, Powder Technology, 153 (2005), pp 43-50

Salman A.D., Gorham D.A., Verba A., Particle–wall impact in dilute pneumatic conveying, Proc. 2nd Israel Conf. Conveying and Handling of Particulate Solids, Jerusalem (1997)

Santos, E.G., Mesquita, A.L.A., Gomes, L.M., Faguri Neto, E., Mafra, M.P., 2012, “Análise da forma geométrica da partícula na aplicação do Método dos Elementos Discretos – DEM” In *Anais do VII Congresso Nacional de Engenharia Mecânica*, São Luís (MA).

Sommerfeld M ., Huber N., Experimental analysis and modelling of particle–wall collisions, International Journal of Multiphase Flow, 25 (1999), pp. 1457-1489

Sommerfeld M ., Huber N., Experimental analysis and modelling of particle–wall collisions, International Journal of Multiphase Flow, 25 (1999), pp. 1457-1489

Zhu, H.P., Zhou, Z.Y., Yang, R.Y., Yu, A.B., 2008, “Discrete particle simulation of particulate systems: a review of major applicattions and findings. Chemical Engineering Science, v.63, no.23, p.5728-5770.